The following resources related to this article are available online at http://stke.sciencemag.org.
This information is current as of 17 June 2012.

RESEARCH ARTICLE

CANCER BIOLOGY

EGF Decreases the Abundance of MicroRNAs That Restrain Oncogenic Transcription Factors

Roi Avraham,[1] Aldema Sas-Chen,[1] Ohad Manor,[2] Israel Steinfeld,[3] Reut Shalgi,[4]*
Gabi Tarcic,[1] Noa Bossel,[5] Amit Zeisel,[5] Ido Amit,[6] Yaara Zwang,[1] Espen Enerly,[7]
Hege G. Russnes,[8] Francesca Biagioni,[9] Marcella Mottolese,[10] Sabrina Strano,[11]
Giovanni Blandino,[9] Anne-Lise Børresen-Dale,[7] Yitzhak Pilpel,[4] Zohar Yakhini,[3,12]
Eran Segal,[2] Yosef Yarden[1]†

Epidermal growth factor (EGF) stimulates cells by launching gene expression programs that are frequently deregulated in cancer. MicroRNAs, which attenuate gene expression by binding complementary regions in messenger RNAs, are broadly implicated in cancer. Using genome-wide approaches, we showed that EGF stimulation initiates a coordinated transcriptional program of microRNAs and transcription factors. The earliest event involved a decrease in the abundance of a subset of 23 microRNAs. This step permitted rapid induction of oncogenic transcription factors, such as c-FOS, encoded by immediate early genes. In line with roles as suppressors of EGF receptor (EGFR) signaling, we report that the abundance of this early subset of microRNAs is decreased in breast and in brain tumors driven by the EGFR or the closely related HER2. These findings identify specific microRNAs as attenuators of growth factor signaling and oncogenesis.

INTRODUCTION

Binding of growth factors to cell surface receptor tyrosine kinases stimulates a network of cytoplasmic events, leading to transcriptional regulation and thereby cell fate decisions (1). For example, stimulation of the mitogen-activated protein kinase (MAPK) pathway is coupled to the rapid induction of transcription factors (TFs) encoded by immediate early genes [IEGs (2, 3)]. Deregulation of signaling cascades downstream of specific growth factor receptors, such as the epidermal growth factor receptor (EGFR), has been implicated in diverse types of human cancer. Moreover, oncogenic transformation is often associated with inappropriate function of components of the network that regulate the amplitude and duration of the EGFR signal through negative feedback. EGFR signaling involves two major mechanisms of feedback regulation, one immediate and one delayed. The immediate wave of feedback regulation, which occurs within 20 min of stimulation, depends on preexisting components of the EGFR signaling network that are translocated, assembled, or altered to achieve stringent control of signals initiated at the cell surface (4). This wave of regulation depends on posttranslational protein modifications, for example, phosphorylation and dephosphorylation (5) or ubiquitination (6). In contrast, the delayed wave of feedback regulation involves newly synthesized proteins, which are encoded primarily by a group of genes collectively called the delayed early genes (DEGs). These include transcriptional repressors and phosphatases (7), which act together to limit the duration of signaling downstream of active receptors (2). One central node of feedback regulation includes TFs encoded by the IEGs, such as members of the c-FOS and c-JUN families of short-lived proteins. Aberrant activation of these well-characterized IEGs, which are rapidly and transiently induced upon mitogenic stimulation (8), is often associated with oncogenic transformation by retroviruses and other agents (9). In contrast, a subset of the DEGs that restrain the transcriptional activation of oncogenic IEGs is commonly down-regulated in tumors, consistent with tumor-suppressive functions (2, 10).

Here, we investigated the possibility that microRNAs, a class of ~22-nucleotide single-stranded RNA molecules that bind to complementary regions in messenger RNA (mRNA) transcripts to inhibit gene expression (11), constitute another layer through which oncogenic signaling networks are regulated. Exactly how mRNAs and their respective microRNAs are integrated into signaling-controlled transcriptional networks is unclear. Moreover, because the target specificity-determining site of microRNAs is often short (seven to eight nucleotides), combinatorial and multiple interactions at each target mRNA may underlie broad regulation of signaling networks by microRNAs (12). MicroRNA regulation in the context of signal attenuation is particularly interesting, because a large body of recent evidence implicates aberrant microRNA expression in most human malignancies (13, 14). Here, we describe mechanisms by which microRNAs may contribute to the oncogenic phenotype. Although we predominantly focused on two aspects of microRNA signaling downstream of EGFR, we also show that similar mechanisms may occur in cancers that are not dependent on EGFR signaling. First, we identified a group of coexpressed microRNAs that showed decreased abundance immediately after EGF stimulation of cultured mammary cells and explored their role in onco-

genesis. We found that these immediately down-regulated microRNAs, together with a group of IEGs that they target, formed a small subnetwork within the complex transcriptional network stimulated by EGF. The primary function of this network is to attenuate IEG expression, thereby controlling the initiation of signal propagation. Second, we identified recognizable modules of microRNAs and mRNAs within the global response to EGF that likely fine-tune transcriptional outcome. We implicate the subset of immediately down-regulated microRNAs in brain and breast cancers, indicating that they act as tumor suppressors by restraining the activity of oncogenic TFs.

RESULTS

EGF elicits an immediate decrease in the abundance of a group of microRNAs that are repressed in tumors driven by EGFR signaling

We stimulated MCF10A mammary epithelial cells (15) with EGF (10 ng/ml) for time intervals ranging between 20 and 480 min and assessed changes in microRNA abundance with oligonucleotide microarrays (Agilent) to investigate the possible roles of microRNAs in signaling downstream of the EGFR. We used a criterion of a factor of >2 change from time zero, over at least two consecutive time points, to consider microRNA abundance significantly altered by EGF stimulation. The resulting matrix (Fig. 1A and table S1) revealed a remarkably dynamic pattern of changes in microRNA abundance over time, which resembled the patterns of changes in mRNA abundance we previously observed after EGF stimulation of MCF10A cells (2). We observed similar dynamic changes in microRNA abundance with EGF stimulation of HeLa human cervical cancer cells (fig. S1B and table S1) and when stimulating MCF10A cells with 5% serum, which contains EGF and other mitogens and induces cell proliferation (fig. S1A and table S1). Experiments with quantitative polymerase chain reaction (qPCR) to analyze selected microRNAs (miR-21, miR-125b, and miR-191) confirmed rapid changes in the abundance of the mature transcripts with EGF stimulation of MCF10A cells (fig. S1C), and further analysis demonstrated successive processing of microRNA precursors (fig. S1D). Likewise, pharmacological analyses confirmed the dependence of changes in microRNA abundance on their de novo transcription and on the catalytic activity of the EGFR (fig. S1E).

The microRNA analyses revealed that a group of 23 microRNAs decreased in abundance by at least 50% within 60 min of stimulation with EGF (hereinafter referred to as the "immediate down-regulated microRNAs," or ID-miRs). To determine whether this simultaneous decrease in multiple ID-miRs occurred under other conditions associated with increased growth factor signaling, we analyzed samples of human tumors showing constitutive EGFR signaling or genetic aberrations of EGFR or the closely related HER2 (see tables S2 and S3 for patient characteristics). The subset of ID-miRs was first analyzed in a data set of microRNAs present in 100 breast cancer specimens. On the basis of matched comparative genomic hybridization (CGH) array data, we divided specimens into two groups: those with amplification of the *EGFR* or *HER2* genes, and those without *EGFR* or *HER2* amplification. We ranked microRNAs according to their differential expression between these two groups (Fig. 1B) and carried out enrichment analysis for the ID-miRs with the use of a minimum-hypergeometric test (mHG, see Supplementary Text). The microRNAs that were decreased in abundance in the *EGFR*- or *HER2*-amplified specimens relative to those without *EGFR* or *HER2* amplification were significantly enriched in the subset of ID-miRs [Fig. 1C and fig. S2A; $P < 1.41 \times 10^{-10}$, mHG test; 15 intermediate-amplification tumors were removed from the analysis]. Consistent with this observation, significant coordinated down-regulation of

ID-miRs was also evident in mammary tumors that overexpressed EGFR, as determined by DNA arrays, relative to those that did not (fig. S2B; mHG test, $P < 3.86 \times 10^{-6}$). We also analyzed samples of
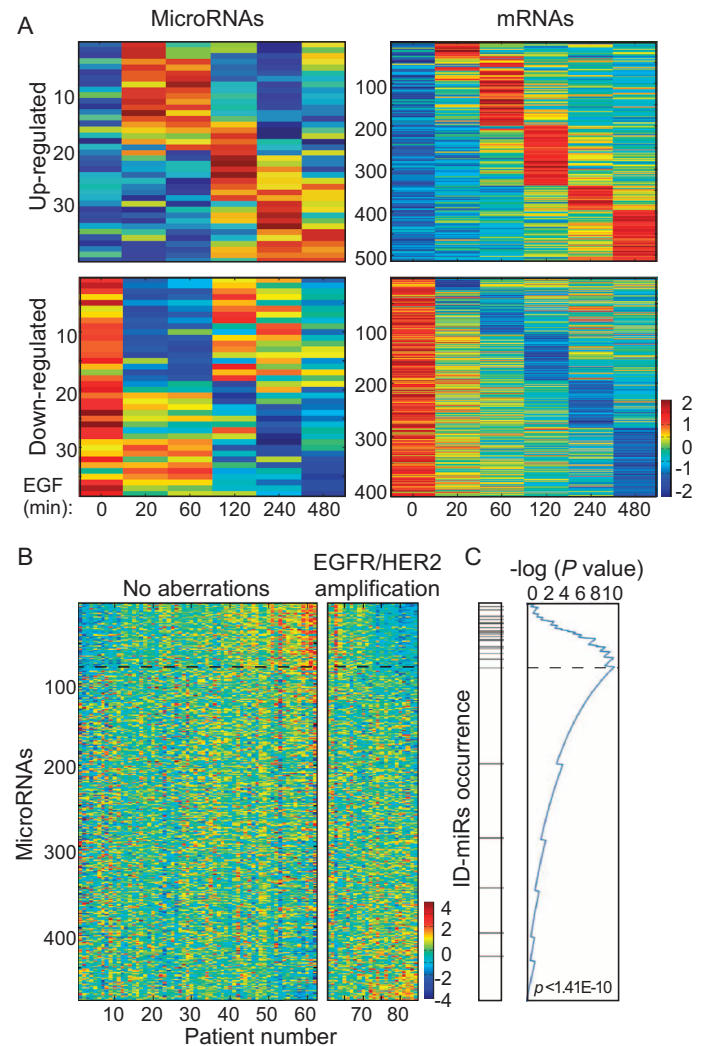
Fig. 1. EGF elicits immediate down-regulation of a group of microRNAs that are specifically repressed in EGFR-driven human breast cancers. (A) Serum-starved MCF10A cells were stimulated with EGF (10 ng/ml) as indicated. RNA was hybridized to a microRNA array (Agilent). MicroRNAs that changed by at least 100% were sorted according to the time of peak abundance (table S1) and compared to the pattern of mRNA induction reanalyzed from (2). (B) MicroRNAs were compared to a breast cancer data set (from 100 patients). Using corresponding CGH data of *EGFR* and *HER2* copy numbers, patients were divided into two groups: no aberration (left) and high (right) copy number of *EGFR* or *HER2*. MicroRNAs were ranked according to a combined *P* value that represents differential expression in amplified versus non-amplified samples (down-regulated microRNAs in amplified samples are shown at the top). (C) The horizontal bars of the left column indicate positions of individual ID-miRs, relative to the ranked heat map of (B). The right column presents the statistical significance of ID-miR distribution within microRNAs that are down-regulated in *EGFR*-amplified samples. The microRNAs that are down-regulated in the tumors are significantly enriched by the subset of ID-miRs ($P < 1.41 \times 10^{-10}$; mHG test).

glioblastoma multiforme (GBM), an aggressive type of brain tumor that often shows amplification of or deletions within the *EGFR* gene [84 patients; The Cancer Genome Atlas (TCGA) compendium (*16*), http://cancergenome.nih.gov/]. As in our analyses of breast tumors, we found that the abundance of the 23 ID-miRs was decreased in GBM tumors with *EGFR* aberrations relative to those without such aberrations (mHG test, $P < 3.01 \times 10^{-9}$; fig. S2, C to E; 19 tumors that showed intermediate *EGFR* amplification were excluded from analysis). Together, these observations with two cell models and two types of human tumors suggested that the abundance of ID-miRs are coordinately decreased by EGFR signaling, both in vitro and in cancer.

The ID-miRs are functionally coupled with EGF-responsive IEGs

Because microRNAs accelerate degradation of their target transcripts, alterations of mRNA abundance might conceivably be coupled to temporal changes in microRNA transcription and degradation (*17*). Indeed, side-by-side comparisons of increases and decreases in the abundance of microRNAs and mRNAs from MCF10A cells reflected similar wave-like configurations (Fig. 1A). To investigate the possible functions of the ID-miRs, we grouped mRNAs that increased in abundance after exposure to EGF according to the time of peak abundance. Using the PITA target prediction algorithm (PITA prediction software, http://genie.weizmann.ac.il/pubs/mir07/mir07_prediction.html) (*18*), we found that mRNAs with peak abundance early after exposure to EGF were more likely to contain ID-miR seed sequences in their 3′ untranslated region (3′UTR) than those that peaked later (Fig. 2A and table S4; see a similar analysis with the Targetscan algorithm in fig. S2F; http://www.targetscan.org/). This suggests that the ID-miR subset regulates early, rather than late, waves of de novo mRNA synthesis. A high-resolution, side-by-side comparison of the temporal expression patterns of microRNAs and mRNAs revealed a negative correlation between ID-miRs and IEGs; that is, mRNAs carrying seed sequences for particular ID-miRs increased in abundance concurrently with repression of those ID-miRs (Fig. 2B).

On the basis of conserved target predictions for the ID-miRs, within the class of IEGs, we constructed a map connecting mRNAs that were targets of specific ID-miRs and increased or decreased in abundance with the same temporal pattern. The map included primarily TFs encoded by IEGs such as c-FOS (putatively targeted by miR-155) and early growth response 1 (EGR1; putatively targeted

by miR-191 and miR-212) (*19*) (Fig. 2B). This subnetwork of ID-miRs and their target IEGs likely gains robustness through internal redundancy (targeting of same IEG by several ID-miRs) and multiplicity (targeting of several IEGs by each ID-miR). Indeed, similar redundant and multiple wirings are common in microRNA networks (*20*), suggesting that although each microRNA offers only mild repression of its target mRNA, overt inhibition of IEGs in resting cells depends on ID-miR redundancy.

To explore the biological relevance of the predicted miR-IEG interactions, we conducted a large screen in which we individually overexpressed each of the 23 ID-miRs in MCF10A cells, which dissociate from epithelial clusters and migrate in response to EGF stimulation (*15*), and determined their effects on cell migration and IEG mRNA abundance (Fig. 3). Real-time qPCR verified a 1000 to 10,000% increase in abundance of the corresponding mature ID-miRs (fig. S3A). Most of the ID-miRs significantly inhibited EGF-induced migration ($P < 0.05$; Fig. 3 and fig. S3B), whereas parallel viability assays indicated that only one ID-miR reduced cell viability (miR-630; by >50%). Although we did not analyze the corresponding proteins, real-time qPCR experiments of 34 of the 43 transcripts targeted by the ID-miRs shown in Fig. 2B indicated that the miR-IEG interactions occurred (Fig. 3 and fig. S3C). Hence, the data presented in Fig. 3 lend experimental support to the proposed network
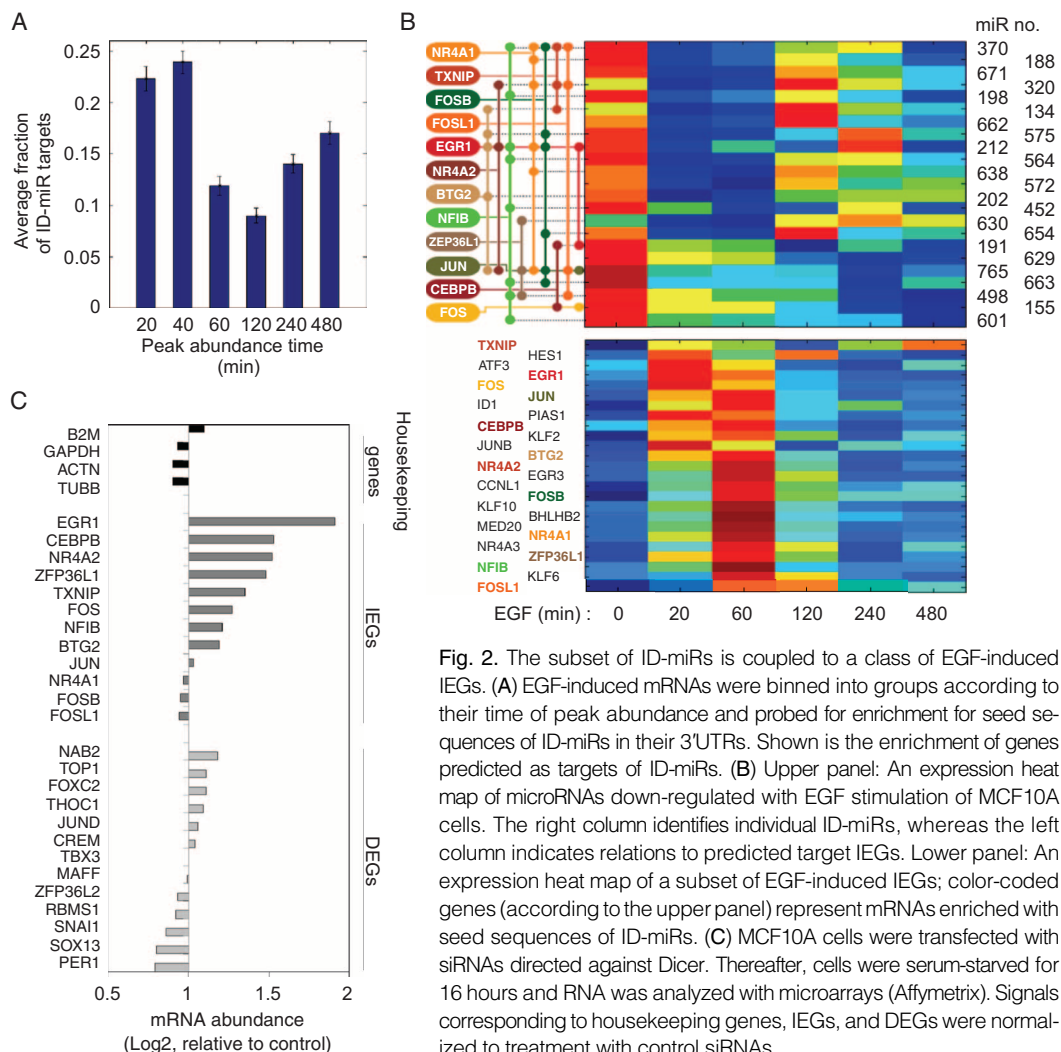
Fig. 2. The subset of ID-miRs is coupled to a class of EGF-induced IEGs. (**A**) EGF-induced mRNAs were binned into groups according to their time of peak abundance and probed for enrichment for seed sequences of ID-miRs in their 3′UTRs. Shown is the enrichment of genes predicted as targets of ID-miRs. (**B**) Upper panel: An expression heat map of microRNAs down-regulated with EGF stimulation of MCF10A cells. The right column identifies individual ID-miRs, whereas the left column indicates relations to predicted target IEGs. Lower panel: An expression heat map of a subset of EGF-induced IEGs; color-coded genes (according to the upper panel) represent mRNAs enriched with seed sequences of ID-miRs. (**C**) MCF10A cells were transfected with siRNAs directed against Dicer. Thereafter, cells were serum-starved for 16 hours and RNA was analyzed with microarrays (Affymetrix). Signals corresponding to housekeeping genes, IEGs, and DEGs were normalized to treatment with control siRNAs.

of ID-miRs and IEGs and identify roles for the ID-miRs in EGF-induced mammary cell migration.

Growth factor–deprived cells show abundant ID-miRs, the predicted targets of which are mitogenic IEGs, often transduced by oncogenic retroviruses [such as viral *FOS* and *JUN* (*21*)]. Thus, we postulated that ID-miRs act as preexisting inhibitors of IEG function. Because our seed sequence analyses predicted that individual IEGs were targeted by multiple ID-miRs (Fig. 2B), testing this model required the simultaneous elimination of multiple microRNAs. Therefore, we knocked down the pre-microRNA–processing endonuclease Dicer (*22*). Gene expression microarrays of unstimulated MCF10A cells identified 447 mRNAs showing increased abundance after Dicer knockdown (table S5). Twenty of the mRNAs induced by Dicer knockdown were included in our data set of EGF-induced genes, suggesting that these mRNAs may be targets of the microRNAs down-regulated by EGF. About half of them (9 of 20) peaked in abundance at early time points after EGF treatment (for instance, the mRNAs encoding FOS and EGR1, which were induced upon knockdown of Dicer; Fig. 2C). In contrast, Dicer knockdown failed to alter the abundance of mRNAs encoded by the DEGs, or four housekeeping genes used as controls. Together, these results confirm attenuation of IEG mRNA abundance by microRNAs and are consistent with studies indicating that promoters of IEGs are poised for activation in resting cells (*23*, *24*).

ID-miRs prevent IEG expression under conditions of growth factor starvation

To investigate the possibility that ID-miRs act as "safeguards" to limit the production of potentially oncogenic IEG-encoded TFs, we focused on the transcription factor EGR1. EGR1, which regulates several tumor suppressors (*9*), was highly induced after Dicer knockdown (Fig. 2C and table S5). The *EGR1* 3′UTR carries seed sequences for miR-191 and miR-212, making it a predicted target for these two ID-miRs [fig. S4A; see also (*25*)]. EGF-stimulated changes in the abundance of miR-191 and miR-212 showed an inverse correlation with those of *EGR1* mRNA (Fig. 4A). Furthermore, microRNA mimics of miR-191 and miR-212 reduced the luminescence of a luciferase reporter containing the *EGR1* 3′UTR, especially when coexpressed. This repression was not apparent with EGR1-luciferase reporters in which single inactivating mutations were introduced into the miR-191 and miR-212 seed sequences (Fig. 4B; mutations are indicated in fig. S4A). The effects of mimic microRNAs on *EGR1* mRNA, along with the effects of an inhibitor of miR-191 on EGR1 abundance (Fig. 4, B and C, respectively), further supported repression of EGR1 by the two ID-miRs (fig. S4A), and prompted us to investigate miR191-EGR1 interaction in more depth. EGR1 abundance showed superinduction after miR-191 knockdown, especially at early time points (Fig. 4C), whereas miR-191 overexpression decreased EGR1 abundance (fig. S4D). Ex-

Fig. 3. List of all ID-miRs and their effects on expression of predicted target IEGs and on EGF-induced migration of mammary cells. ID-miRs are ordered according to the time of their lowest peak in abundance after EGF stimulation in MCF10A cells. Abundance in MCF10A and in HeLa cells was determined (table S1; N.E., not expressed; "–," no change in abundance, "↓," at least a 50% decrease from time zero). For assessment of migration, MCF10A cells were transfected with either control oligonucleotides and pre-miR expression plasmids, the indicated microRNA mimic oligonucleotides, or pre-microRNA expression plasmids, and migration was assessed with a Transwell assay (Materials and Methods). Horizontal bars indicate means and SD values (in percentages) compared to control transfections (the gray area indicates the range of migration in three independent control transfection experiments). The experiment was repeated twice for each ID-miR. For assessment of effects on predicted target genes, MCF10A cells were stimulated with EGF for 0, 30, or 60 min. Thereafter, mRNA abundance of the indicated target IEGs was analyzed with real-time qPCR. Signals were quantified relative to three independent control mRNAs [B2M, tubulin, and GAPDH (glyceraldehyde-3-phosphate dehydrogenase)]. The heat map presents change in abundance of target genes relative to control transfections.
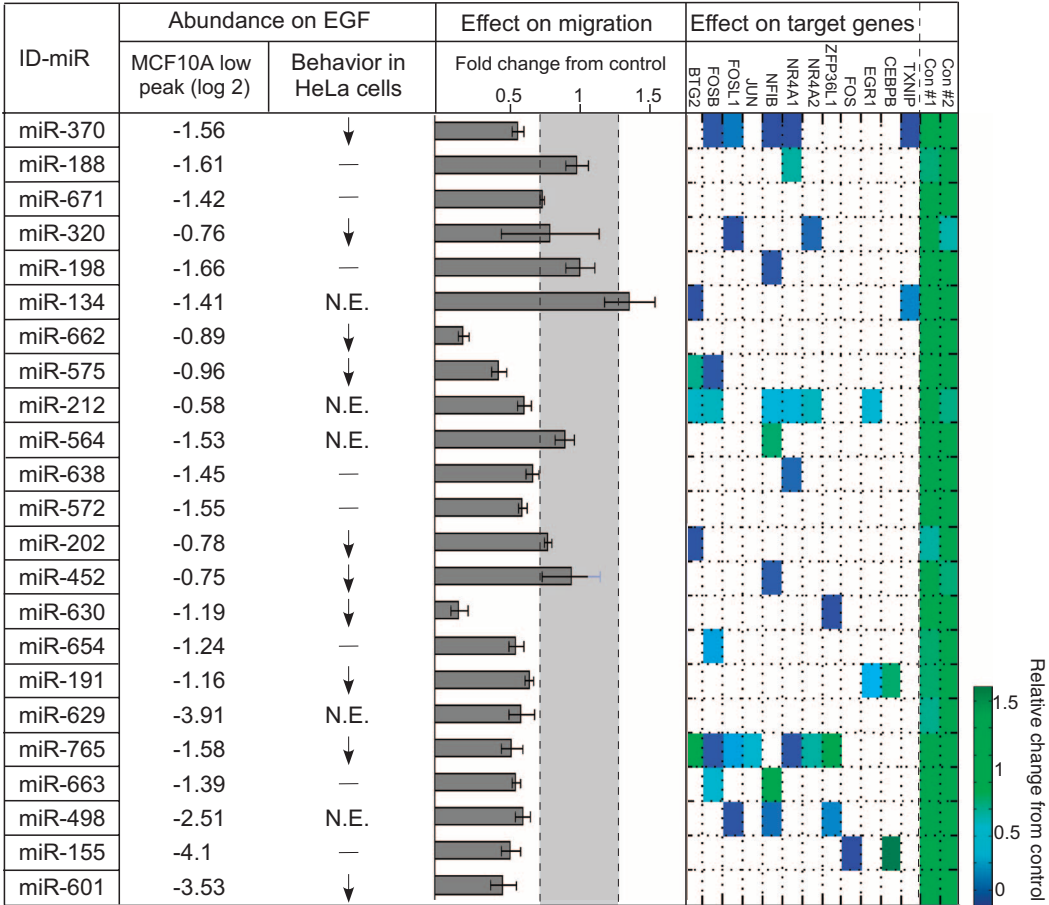
periments with an miR-191 inhibitor indicated that miR-191 inhibits the transcription of EGR1 target genes in both resting and EGF-stimulated cells (Fig. 4D).

We next tested the effect of the predicted miR191-EGR1 interaction on two functional sequelae of EGF stimulation: MCF10A cell migration and human mammary epithelial cell (HMEC) proliferation. miR-191 knockdown increased EGF-dependent migration in a Transwell assay, an effect that was nearly abolished by simultaneous EGR1 knockdown (Fig. 4E and fig. S4E). This suggests that the decrease in miR-191 abundance in response to EGF stimulation may induce migration by releasing inhibition of EGR1. A wound-healing assay, which assesses cell migration, revealed the ability of ID-miRs to discriminate between substantial from insubstantial signals: At high concentrations (10 ng/ml), EGF induced robust wound closure, an effect that was hardly detectable at 0.1 ng/ml (Fig. 4F). With miR-191 knockdown, however, cell migration was apparent at an EGF concentration of 0.1 ng/ml. HMECs, unlike MCF10A cells, undergo proliferation after treatment with EGF, and miR-191 knockdown in these cells increased EGF-induced proliferation (fig. S4F). Thus, we propose that under conditions of growth factor deprivation, miR-191 and

miR-212 are abundant, thereby preventing *EGR1* expression, but that, after EGF stimulation and the ensuing decrease in ID-miR abundance, EGR1 production increases, promoting cellular proliferation and migration (Fig. 4G).

The viral oncogene v-*FOS* escapes regulation by ID-miRs

Aberrant forms of several IEGs act as retroviral transforming genes. For instance, the Finkel-Biskis-Jinkins (FBJ) murine osteosarcoma virus captured most of the coding region of the c-*FOS* gene (*26*) and thereby acquired the ability to transform cells. Given the oncogenic capacity of v-*FOS*, we postulated the existence of viral mechanisms allowing it to evade regulation by ID-miRs. We compared its sequence to that of its cellular counterpart, c-*FOS*, and noted that their 3′UTRs differed (Fig. 5A), although the 3′UTR of c-*FOS* is highly conserved (Fig. 5B). Our analyses of MCF10A and HeLa cells identified miR-155 and miR-101, both of which regulate c-*FOS* (*26*, *27*), as ID-miRs. Notably, the miR-155 seed-binding site of v-*FOS* carried a central region mutation, and the seed-binding site for miR-101 was deleted. We found that ectopic expression
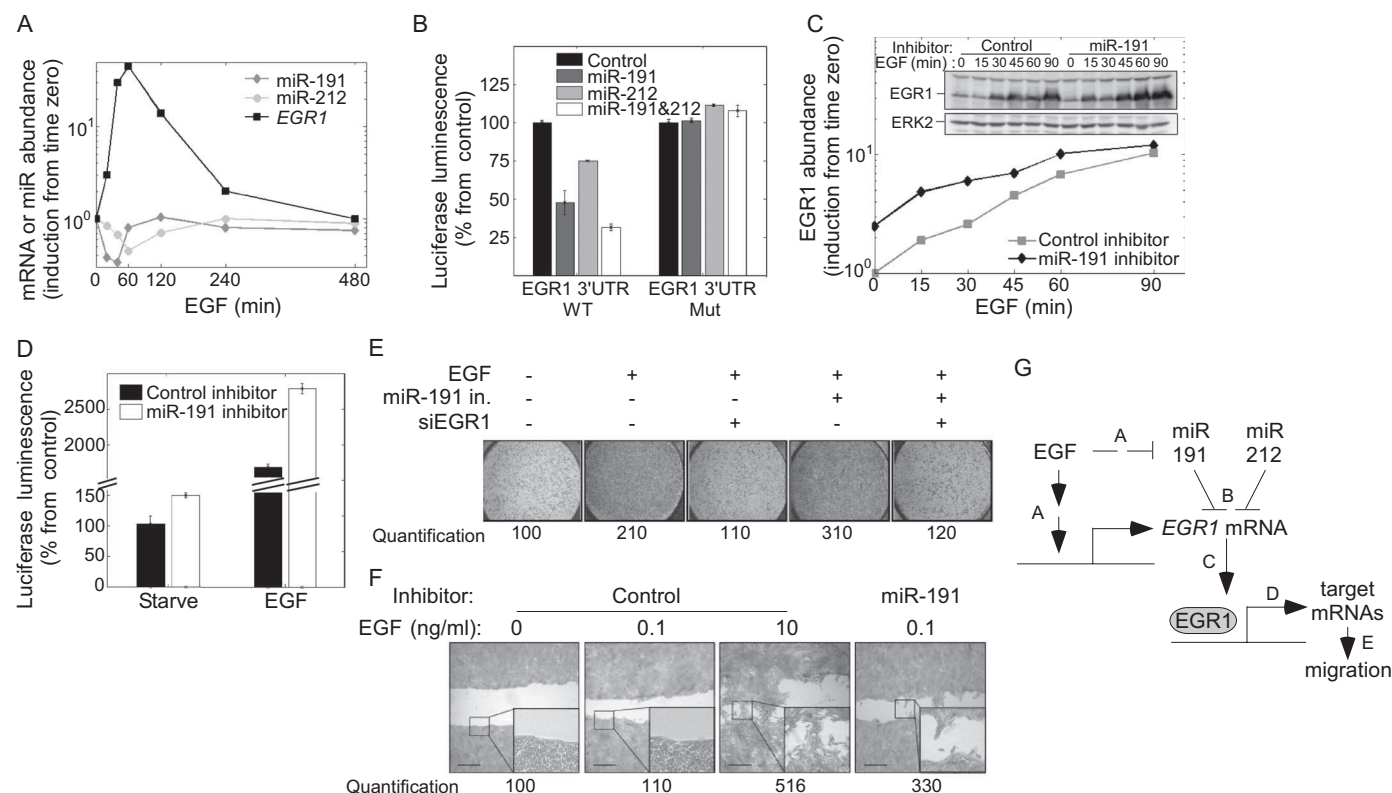
Fig. 4. ID-miRs prevent IEG expression under conditions of growth factor deprivation. (**A**) RNA from EGF-treated MCF10A cells was analyzed with real-time qPCR. (**B**) HeLa cells were cotransfected with specific microRNA mimics and either a luciferase reporter containing wild-type 3′UTR of *EGR1* or one with an *EGR1* 3′UTR with mutations in the seed sequences (see fig. S4A). Means and SD values of duplicates luminescence signals are presented. (**C**) MCF10A cells were transfected as indicated and then stimulated with EGF and analyzed by immunoblotting. Normalized signals are presented, along with the original blot (inset). (**D**) HeLa cells were transfected as indicated. A luciferase reporter gene driven by a promoter containing an EGR1-responsive element was introduced; 40 hours later, serum-starved cells were stimulated with EGF for 4 hours. (**E**) MCF10A cells were transfected with either control, miR-191–specific, or EGR1-specific oligonucleotide inhibitors (alone or in combination, as indicated). Thereafter, migration was assessed with a Transwell assay (see Materials and Methods); signals were normalized to control and shown below each panel. (**F**) MCF10A cells were transfected as in (C). Thereafter, migration was assessed with a wound closure assay (see Materials and Methods); scale bar, 100 μm; insets: 20× magnification. (**G**) A summary scheme showing the effects of EGF on miR-191, miR-212, and EGR1. Letters refer to specific panels of the figure.

of miR-101, as well as miR-155, reduced luminescence signals emanating from a reporter carrying the 3′UTR of c-*FOS*. In contrast, neither miR-101 nor miR-155 altered signals from a reporter bearing the v-*FOS* 3′UTR (Fig. 5C). The 3′UTR of c-*FOS* contains, in addition to ID-miR seed sites, AU-rich elements that are recognized by RNA-binding proteins that regulate mRNA stability, such as the zinc finger protein 36 (ZFP36) (*28*). Accordingly, we observed that, whereas the increase in abundance of c-*FOS* mRNA in response to EGF or serum is coupled to a decrease in abundance of miR-155 and miR-101, the decrease in abundance of c-*FOS* mRNA correlated with the delayed induction of ZFP36 (Fig. 5D). Thus, we conclude that increased v-FOS stability resulting from the loss of ZFP36 binding sites (*26*) and ID-miR seed sites likely contributes to prolonged activation of downstream c-FOS target genes.

ID-miR abundance can distinguish between malignant and surrounding tissues

The differential ability of the ID-miRs to regulate v-FOS and c-FOS, along with other oncogenic IEGs, suggested that low abundance of ID-miRs may serve as a predictor of pathological states. To investigate this possibility, we stratified the breast cancer tumors described in Fig. 1B according to their clinical subtype, which serves as an indicator of aggressiveness of the tumor (*29*). We found that the more aggressive types of tumors (HER2^{+}, basal-like, and luminal B) showed decreased ID-miR abundance relative to less aggressive lesions (luminal A and normal-like; Fig. 6A, paired t test, $P < 2 \times 10^{-10}$). We further studied the correlation in abundance between ID-miRs and IEGs in these samples and found a trend of negative correlation, but this was not statistically significant (see table S6). A comparison of tumors and adjacent normal tissue (peritumor) from a separate cohort of 58 breast cancer patients (Fig. 6B and table S3) revealed that 19 of 23 ID-miRs were coordinately and significantly down-regulated in tumors relative to

their matched peritumors [Fig. 6C; Gene Set Enrichment Analysis (*30*, *31*) http://www.broadinstitute.org/gsea/, $P < 0.0001$]. Together, these observations suggest that breast tumors uncouple a cascade linking ID-miRs and IEGs, as well as DEGs (*2*), which normally controls the sharp peak in IEG abundance after stimulation with EGF, and thereby defines the boundaries of the active cellular state (Fig. 6D; see Discussion).

The global transcriptional response to EGF involves multiple modules of microRNAs and TFs co-regulating a common target mRNA

Two striking features of the ID-miR–IEG network were that each ID-miR was predicted to target multiple IEGs and that a collective decrease in ID-miR abundance coincided with the transcriptional induction of an IEG. The first feature is demonstrated in Fig. 3, where ectopic expression of individual ID-miRs caused a decrease in the abundance of several predicted IEG targets, illustrating that these ID-miRs had multiple targets. A specific example of this, involving overexpression of miR-765, is presented in Fig. 7A. This multiplicity of ID-miR targets, represented in the schematic shown in Fig. 7B, was extended beyond the ID-miR and IEG domain by surveying all EGF-regulated mRNAs and microRNAs in MCF10A cells. For this global analysis, we developed a computational tool aimed at multiple analyses of predicted microRNA-mRNA pairs. For each microRNA, we compiled two mRNA lists ordered by (i) prediction score of conserved mRNA targets (with TargetScan and PITA prediction algorithms), and (ii) correlation between the abundance profile of the microRNA and the abundance profile of all mRNAs in our data sets. We found significant correlation (or anticorrelation) between the abundance profile of microRNAs altered in response to EGF and of the respective sets of predicted target mRNAs (see global analysis for both MCF10A and HeLa cells in fig. S5A).
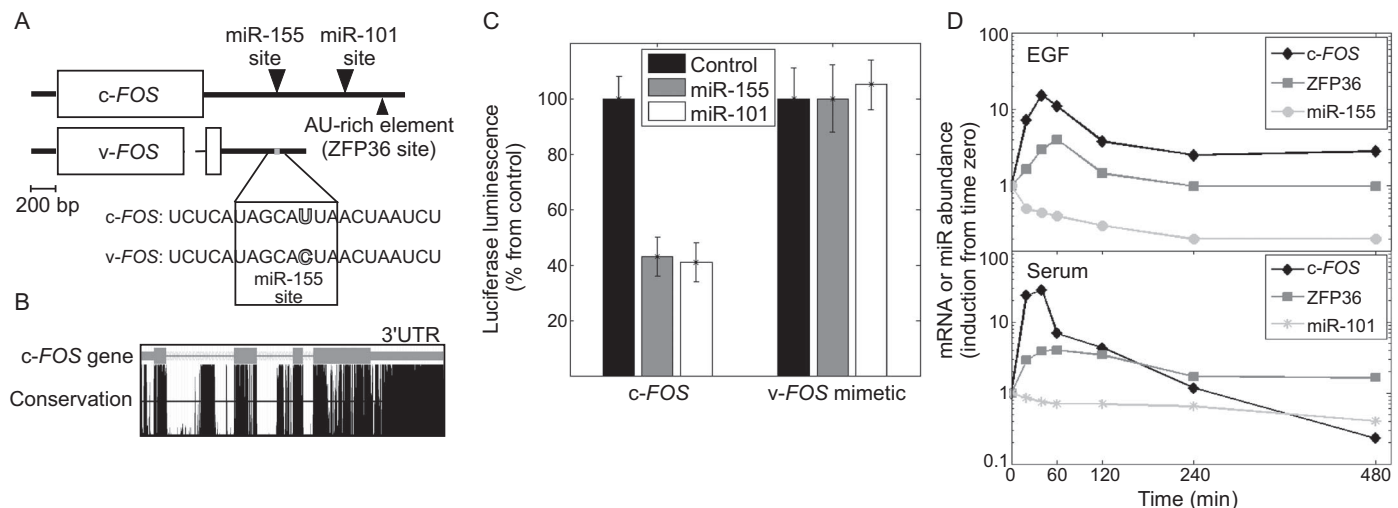
Fig. 5. The viral oncogene v-*FOS* escapes regulation by ID-miRs. (**A**) Illustration and sequences of c-*FOS* and v-*FOS* transcripts, including binding sites for ID-miRs and ZFP36. Note a single base replacement within the shorter 3′UTR of the v-*FOS* transcript. (**B**) Upper panel: the exon-intron structure of the c-*FOS* gene, with exons indicated by thick lines and introns indicated by thin lines. Lower panel: histogram (obtained with the UCSC Genome Browser; http://genome.ucsc.edu/) indicates the degree of conservation of the corresponding regions between all vertebrate forms of c-*FOS*. Note that the tail of the 3′UTR of c-FOS is among the most conserved parts. (**C**) HeLa cells were cotransfected with a pre-miR–encoding plasmid (Control, miR-155, or miR-101) and a luciferase reporter (the 3′UTR of c-*FOS* or a v-*FOS* mimetic bearing the corresponding truncation and mutation). Luminescence was measured 48 hours later. Means and SD values (bars) of duplicates of three repeats are presented. (**D**) MCF10A cells were treated with EGF (10 ng/ml) or with serum (5%) for the indicated time intervals. RNA was analyzed by real-time qPCR with primers corresponding to the indicated transcripts.

Plotting the average correlation of each microRNA to its predicted targets, compared to random gene sets, reflected comprehensive and significant correlations between microRNAs and groups of their predicted target transcripts (Fig. 7C and table S7). We could observe a small trend for correlation with the random gene sets, as they also contain targets. We next tested the biological relevance of these correlations. MCF10A cells show a differential response to EGF and serum: They migrate in response to EGF but proliferate in response to serum factors (fig. S5B). Intriguingly, the sets of predicted targets showing significant correlation to EGF- or to serum-responsive microRNAs corresponded to Gene Ontology (Gene Ontology database: http://www.geneontology.org, DAVID: functional annotation tool: http://david.abcc.ncifcrf.gov/summary.jsp) categories of cell adhesion and proliferation, respectively (fig. S5C). These observations uncover outcome-specific, extensive coordination between the inducible microRNAs and the expression of their target transcripts.

The other feature of the ID-miR–mRNA network we investigated, both locally and globally, was the coordinated transcriptional induction

of IEGs. An example of this is shown in Fig. 7D: Whereas EGF induces up-regulation of c-FOS through the activation of an upstream TF [such as the serum response factor (SRF)], at least two EGF-regulated ID-miRs control c-FOS abundance (miR-155 and miR-101). The corresponding circuitry is depicted in Fig. 7E: EGF induces transcription of an IEG through the activation of a constitutive TF; on the other hand, it down-regulates a group of ID-miRs targeting the same IEG, in line with recurrence of similar motifs in transcriptional networks (32). To identify such EGF-inducible motifs, we used a previously compiled list of pairs of microRNAs and TFs (33). We focused on pairs sharing a large set of common target genes (where the TF has a conserved binding site in the promoter of the target, and the microRNA has a conserved predicted seed site in the respective 3′UTR of the mRNA; which we call co-occurring miR-TF pairs) and analyzed them for correlation in their EGF-dependent abundance in our data sets. Plotting the expression correlation for each predicted miR-TF pair, compared to random TF sets, reflected comprehensive and significant correlations (Fig. 7F and table S8).

Fig. 6. Abundance of ID-miRs correlates with malignancy of breast lesions. (A) The database of breast cancer (Fig. 1B) was analyzed for ID-miR abundance according to disease subtypes. Green lines represent group overall averages. (B) MicroRNAs were analyzed against a patient data set containing pairs of breast tumor and the adjacent tissue (peritumor; 58 patients). Shown is a heat map representing abundance ratio of microRNA between tumors and matched peritumors; microRNAs were sorted according to a combined P value (see Materials and Methods) that represented average relative change. (C) The blue bars of the left column indicate positions of individual ID-miRs relative to (B). The right column presents an enrichment curve of the ID-miRs (blue line; enrichment score = 0.71) in comparison to random permutations (gray area; the dashed line indicates mean of enrichment scores of randomly selected groups of microRNAs). (D) A scheme showing cyclic transitions between a resting cellular state (arrest) and an active state comprising binary switches able to control IEGs. The switches involve immediate down-regulated microRNAs (ID-miRs), as well as DEGs (for instance, ZFP36, and a MAPK phosphatase, DUSP6). The cycle is initiated by an extracellular stimulus, such as EGF. A.U., arbitrary units of abundance.

This analysis revealed that the abundance of microRNAs up-regulated by EGF correlated with the abundance of their putative TF co-regulators (fig. S6, A to C, and table S7). In contrast, the down-regulated microRNAs tended to negatively correlate with their co-occurring TFs (fig. S6, D to F). These co-occurring miR-TF pairs are embedded in the network as part of generic feed-forward loops [FFLs (34)]. As an example of a FFL, we analyzed one coherent and one incoherent module [respectively defined as modules in which the path from EGF to the target gene bifurcates into two pathways, whose overall signs (inhibition or induction) are either identical or opposite] (figs. S6B and S6E, respectively). An incoherent module, such as miR-183 and the TF C/EBP, involves positive correlation between a microRNA and a TF, which enables microRNAs to act as rheostats that tune the output of protein production (35). Coherent modules, however, involve negative correlation between a microRNA and a TF, so that EGF inhibits the expression of a microRNA, but increases the abundance of the TF. This type of regulation likely incorporates on-off transcriptional switches in the global response to EGF (36). As an example, we show a coherent, EGF-induced module consisting of miR-320 and the TF CREM (cyclic adenosine 3′,5′-monophosphate responsive element modulator).

In summary, our study identified microRNAs as an essential component of the transcriptional response of cells to growth factors. Along with extensive coordination of the transcriptional response at the network level, our global analyses uncovered generic modules of microRNAs and TFs that co-regulate the same target transcripts. Because the ID-miR–IEG axis emerged from our surveys of clinical data as a general target of collective aberrations frequently identified in breast and brain tumors, we assume that further studies of the global transcriptional response to EGF will unveil more subnetworks relevant to human diseases.

DISCUSSION

Unlike the well-characterized roles for newly synthesized mRNA molecules in short- and long-term cellular responses to growth factors, roles for microRNAs are only just emerging. The importance of such regulation is exemplified by miR-7 and Yan, the TF it regulates, in EGF-mediated control of insect eye development (37), but no global analysis has previously been performed. Our data argue that the two transcriptional arms of EGFR signaling, EGF-induced microRNAs and mRNAs, are similarly dynamic and subtle (Fig. 1A) and show extensive mutual coordination at the systems level (Fig. 7) (38). Experiments in *Caenorhabditis elegans* indicate that redundancy among closely related microRNA family members underlies the milder effects of deleting individual microRNA loci compared with the more severe effects of deleting individual TFs (39). This
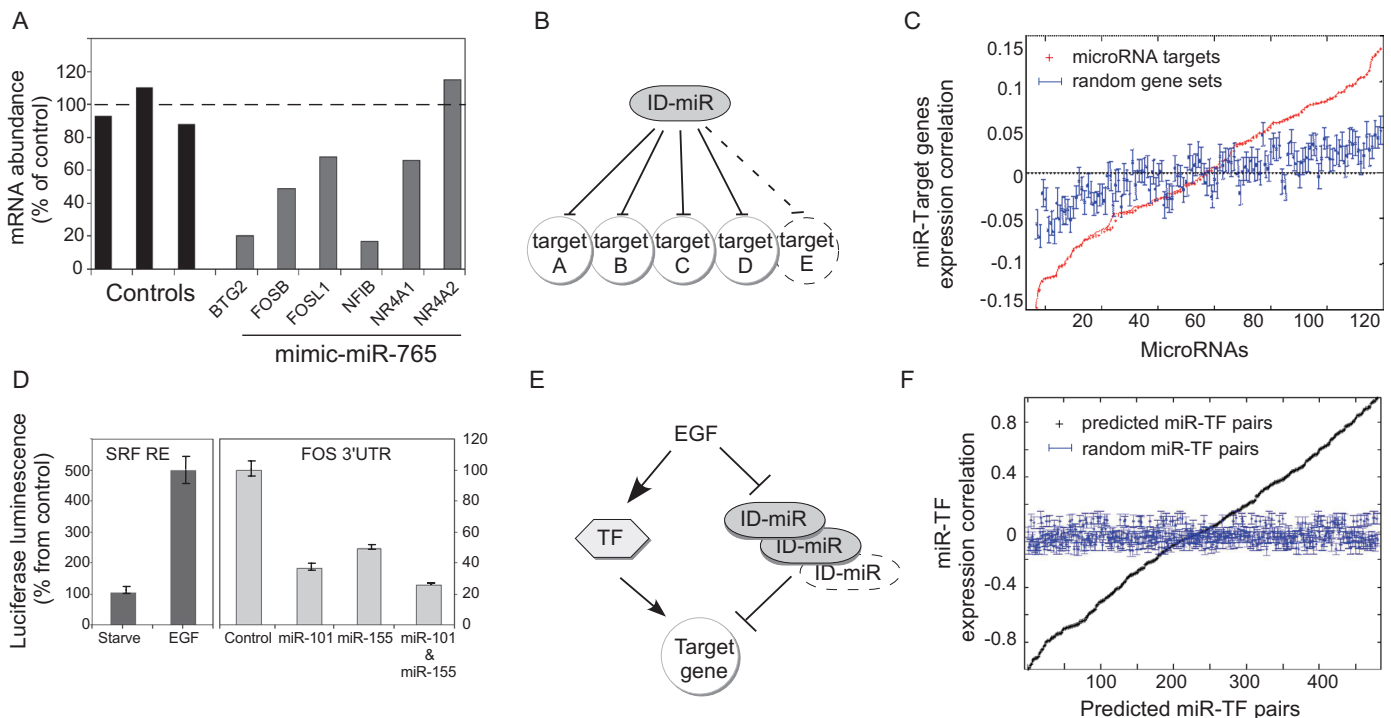

Fig. 7. Responses to growth factors involve a cascade of ID-miRs, transcription factors, and multiple target genes. (**A**) MCF10A cells were transfected as indicated and RNA was analyzed by real-time qPCR with primers for the indicated putative target mRNAs of miR-765 (actin, GAPDH, and tubulin served as controls). (**B**) Schematic depiction of the multiple genes targeted by each ID-miR. A dashed circle indicates additional targets. (**C**) Analysis of correlations of expressions between EGF-regulated microRNAs and their predicted target mRNA groups. Each entry reflects an expression correlation between an EGF-regulated microRNA and either a random gene set (blue) or the respective predicted targets (red). (**D**) Left panel: HeLa cells were transfected with a luciferase reporter containing a promoter with SRF response element (RE). Thereafter, serum-starved cells were stimulated with EGF and luminescence was assessed. Right panel: HeLa cells were cotransfected with the indicated pre-miR–encoding plasmids, along with a luciferase reporter of the c-*FOS* 3′UTR. Luminescence was measured 48 hours later. (**E**) Schematic representation of EGF-regulated microRNAs and TFs that converge on target genes. (**F**) Analysis of co-occurring miR-TF pairs regulating common mRNA targets. Each entry reflects the correlation of abundance between an EGF-regulated microRNA and either a predicted co-occurring TF (black) or random TF sets (blue; see table S8).

redundancy has raised the possibility that the effect of microRNAs on developmental and signaling processes may be more restricted than that of TFs (*32*). Along with fine-tuning the transcriptional signals carried out by TFs, microRNAs have unique features that may enhance the versatility of signaling pathways. These features include the ability to terminate gene expression more rapidly than transcriptional repressors can, along with localized action at ribosomes (*40*).

To uncover unique features of microRNAs and their links to target transcripts, we compared the patterns of inducible mRNAs and microRNAs after stimulation with EGF and serum. This enabled us to integrate data on all the inducible microRNAs and mRNAs. Targets of microRNAs can be predicted above the background of false positives by searching for conserved matches to the seed region (*12*). Because microRNAs instigate degradation of their target transcripts, the spectrum of correlations of abundance profiles of microRNAs with their target mRNAs is expected to be negative (*17*). Nevertheless, some studies have shown coexpression of a microRNA and the target mRNA (*35*). Accordingly, the genome-wide survey we performed with EGF-stimulated cells revealed both negative and positive correlations between microRNAs and target mRNAs. We propose that this broad spectrum of correlations reflects functions beyond binary switches and is related to the fine-tuning of signaling pathways. Along with the extensive interaction between microRNAs and mRNAs induced by EGF, we also examined network motifs consisting of a TF and a microRNA. We found many coherent and incoherent motifs in which a microRNA-TF pair co-regulates a target gene. The multiplicity of such modules has previously been uncovered by a wide-scale computational analysis of mammalian regulatory networks (*33*). Conceivably, incorporation of these modules in the EGFR signaling system enhances control and finely tunes the output.

One striking feature of the pattern of EGF-responsive microRNAs we observed was the rapid decrease in abundance of a group of microRNAs we called ID-miRs. Genes that are coordinately expressed often share similar cellular functions (*41*, *42*). Applying this concept to microRNAs, we showed that these coexpressed ID-miRs coordinately targeted IEG transcripts that share a cellular function in initiating the response to a variety of extracellular stimuli, such as mitogens and stress inducers. Using resting cells and suboptimal EGF concentrations, we further demonstrated that the ID-miRs constitute a subnetwork, which ensures that IEGs are kept repressed before stimulation by an extracellular stimulus. In support of this scenario, several studies have recently indicated basally active, yet nonproductive transcription of IEGs in resting cells (*23*, *24*, *43*). The biochemical basis of the rapid and selective down-regulation of ID-miRs by EGF remains unknown. However, this group of microRNAs is also down-regulated in patients with brain or breast tumors harboring genomic aberrations in the EGF receptor (Fig. 1 and fig. S2C), which implies that the unknown biochemical pathways are clinically important. Although little is known about the mechanisms mediating microRNA degradation in vertebrates, a recent study identified a family of exoribonucleases capable of degrading mature microRNAs in *Arabidopsis thaliana* and concluded that microRNA turnover is crucial for plant development (*44*).

RNA degradation is also regulated by several DEG products, a class of negative regulators responsible for the short half-life of most IEG-encoded transcripts (*2*). Thus, ID-miRs and DEGs determine the steeply shaped profile of IEG expression in healthy cells (Fig. 6D). In contrast, deviations from pulsed expression of IEGs appear to underlie pathogenic situations, such as infection by transforming RNA retroviruses [for instance, the lethal osteosarcomas induced by v-FOS–encoding FBJ-MSV and FBR-MSV murine viruses; (*21*)]. We speculated that the ability of ID-miRs to discriminate substantial from insubstantial stimuli (Fig. 4F) might be exploited in early steps of pathogenesis as a mechanism of hypersensitivity to growth factors.

Indeed, we demonstrated that the viral oncogene, v-*FOS*, evades regulation by two ID-miRs (Fig. 5). Moreover, a substantial proportion of the ID-miR group is down-regulated in breast tumors compared to adjacent normal tissue, and they can collectively serve as indicators of a disease state (Fig. 6). Previous analyses of microRNAs in tumors have reported alterations in expression of individual ID-miRs; however, their collective behavior and relevance to the group of IEGs have escaped detection. Examples include down-regulation of miR-101 in hepatocellular carcinoma (*27*), hypermethylation of miR-370 in cancer cells (*45*), loss of miR-320 in several tumors (*46*), as well as hypermethylation of miR-663 in breast cancer patients (*47*).

In summary, we provide strong evidence in favor of a role for EGF-inducible microRNAs as components of a remarkably dynamic and subtle transcriptional program, which is well coordinated with the mRNA arm. Specifically, we uncovered an early subnetwork, the ID-miRs, that represses expression of TFs. Evidence we obtained in vitro and data derived from clinical specimens indicate that the group of ID-miRs counterbalances oncogenic TFs, but this safeguard mechanism is defective in cancer. The pattern of EGF-regulated early microRNAs we described herein, along with recent studies, which concentrated on individual microRNAs and utilized transforming growth factor–β (*48*, *49*) or estradiol (*50*), suggest that a combinatorial code of microRNAs underlies robust responses to extracellular stimuli. It remains for future studies to resolve the roles of the delayed phase of inducible microRNAs, thereby uncovering the full effect of the microRNA-mRNA nexus on signal transduction and oncogenesis.

MATERIALS AND METHODS

Statistical analysis, including analyses of patients, is included in the supplementary text.

Cell lines and RNA preparation

MCF10A cells were grown in Dulbecco's modified Eagle's medium–F12 (DMEM-F12) supplemented with antibiotics, insulin (10 mg/ml), cholera toxin (0.1 mg/ml), hydrocortisone (0.5 mg/ml), heat-inactivated horse serum [5% (vol/vol); Gibco BRL], defined as "serum" in the text, and EGF (10 ng/ml). E184A1 HMEC cells were grown in medium containing EGF and pituitary extract. HeLa cells were grown in DMEM (Gibco BRL) supplemented with 10% heat-inactivated fetal bovine serum (Gibco BRL), 1 mM sodium pyruvate, and a penicillin (100 U/ml)–streptomycin (0.1 mg/ml) mixture (Beit Haemek, Israel).

Real-time quantitative PCR and oligonucleotide microarray hybridization

MicroRNA abundance. Complementary DNA (cDNA) was generated with Qiagen's miScript kit. Real-time qPCR analysis was performed with SYBR Green I (Qiagen). Primers were designed according to the mature microRNA sequence (miRBase, Sanger Institute release 11.0, http://microrna.sanger.ac.uk/sequences/index.shtml). Total RNA (100 ng) was labeled and hybridized to Human miRNA Microarray V1 (Agilent). The expression value for each microRNA was calculated with Feature Extraction software 9.5.1. MicroRNAs that were not detected in more than three time points according to GeneView flags were removed. All values lower than 5 were leveled to 5. For each microRNA the intensity values were normalized across the sample set.

mRNA abundance. cDNA was generated by the use of SSII reverse transcriptase (Invitrogen). Real-time qPCR analysis was performed with SYBR Green I (Finnzymes, Invitrogen) as a fluorescent dye. Primers were designed with UniversalProbeLibrary (http://www.roche-applied-science. com/sis/rtpcr/upl/ezhome.html; see table S9 for a list of primers), and β2 microglobulin (B2M) served for normalization. Analysis of oligonucleotide

microarrays after Dicer knockout was performed as follows: RNA (300 ng) was hybridized to human GeneST 1.0 array (Affymetrix) according to the manufacturer's instructions. After the arrays were scanned, the expression of each gene was calculated with Affymetrix Microarray software 5.0 (MAS5).

Lysate preparation and immunoblotting analyses

Cells were scraped in solubilization buffer [50 mM Hepes (pH 7.5), 150 mM NaCl, 10% glycerol, 1% Triton X-100, 1 mM EDTA, 1 mM EGTA, 10 mM NaF, 30 mM β-glycerol phosphate, 0.2 mM Na_3VO_4 and a protease inhibitor cocktail]. Boiled lysates were subjected to SDS–polyacrylamide gel electrophoresis (SDS-PAGE), followed by electrophoretic transfer to a nitrocellulose membrane. After transfer, nitrocellulose membranes were blocked in TBST buffer [0.02 M tris-HCl (pH 7.5), 0.15 M NaCl, and 0.05% Tween 20] containing 10% low-fat milk, blotted for 12 hours with a primary antibody, washed with TBST (tris-buffered saline–Tween 20), and incubated for 30 min with a secondary antibody linked to horseradish peroxidase (HRP).

Wound closure assay

MCF10A cells were grown to 100% confluence in 12-well plates, and then a strip of cells was removed with a sterile pipette tip. The strip was immediately marked and photographed at 20× magnification for quantification. Cells were then incubated for 16 hours with EGF, fixed with 100% methanol, and photographed at 20× magnification in the same locations. Wound closure was calculated as the differential area covered before and after the incubation.

Transwell cell migration assay

Cells were plated in the upper compartment of a Transwell tray (Corning) and allowed to migrate through an intervening nitrocellulose membrane for 20 hours at 37°C. The membrane was then removed and fixed in para-formaldehyde (3%), followed by cell permeabilization in Triton X-100 and staining with methyl violet. Cells growing on the upper side of the membrane were scraped with a cotton swab, and cells growing on the bottom side of the membrane were photographed and then disintegrated in 10% acetic acid for quantification.

MTT viability assay

Cell viability (survival) was determined by applying a 2 hour–long incubation with 3-(4,5-dimethylthiazol-2-yl)-2,5-diphenyltetrazolium bromide (MTT), followed by lysis in acidic isopropanol (0.35% HCl in isopropanol) and measurement of absorbance at 570 nm. The assay was carried out in sextuplets.

BrdU incorporation assay

E184A1 cells were seeded in medium containing EGF and pituitary extract. Twenty-four hours later, cells were transfected with the indicated small interfering RNA (siRNA) oligonucleotides by HiPerfFect (Qiagen GmbH). Cells were replated on coverslips (120 × 10³ cells per well) in full medium 24 hours after transfection. Twenty-four hours later, cells were starved for 16 hours. Thereafter, the cells were incubated for 9 hours without or with EGF (10 ng/ml), then washed and incubated for 3 hours with a 5-bromo-2′-deoxyuridine (BrdU)–labeling reagent, after which they were fixed and stained for BrdU. BrdU and DAPI (4′,6-diamidino-2-phenylindole)–stained nuclei were counted in 14 fields of each slide.

Expression vectors and siRNAs

All plasmids encoding pre-miRs were from R. Agami (The Netherlands Cancer Institute), pRL-TK with EGR1 3′UTR from J. Nielson, psi-CHECK2 with c-FOS 3′UTR from H. J. Lee (NIH, Bethesda, MD). siRNA oligo-

nucleotide pools directed at dicer, EGR1, and all microRNA inhibitors were purchased from Dharmacon. All microRNA mimics (synthetic oligonucleotides that act as mature microRNAs; the numbers of miRs we used were as follows: 212, 188, 198, 671, 662, 575, 564, 638, 572, 654, 629, 765, 663, and 601) were purchased from Qiagen.

Luciferase reporter assays

For 3′UTR reporter assays of c-FOS, cells were cotransfected with JetPEI (Polyplus-transfection) with a wild-type c-FOS 3′UTR or a v-FOS mimetic along with the indicated combinations of expression plasmids. For 3′UTR reporter assays of EGR1, cells were cotransfected with reporter plasmids encoding a wild-type EGR1 3′UTR or a 3′UTR with mutations in the miR-191 and miR-212 seed sequences and a pGL3-CMV containing Firefly luciferase (Promega). Cells were also transfected with microRNA mimic oligonucleotides (Qiagen) of miR-191, miR-212. In both assays, 48 hours after transfection with the reporter plasmid, cells were harvested and Firefly and Renilla luciferase activities were measured with the Promega dual-luciferase assay system. For promoter element assays, HeLa cells were transfected with JetPEI (Polyplus-transfection) with plasmids encoding response elements of NFκB (nuclear factor κB) and either EGR1 or SRF, fused to a luciferase reporter gene.

SUPPLEMENTARY MATERIALS

www.sciencesignaling.org/cgi/content/full/3/124/ra43/DC1
Supplementary Text: Statistical Analysis, including analyses of patients.
Fig. S1. Dynamic alterations of microRNA abundance after stimulation with EGF or serum.
Fig. S2. EGF-regulated microRNAs associate with specific subsets of two tumor types.
Fig. S3. Effects of ID-miR overexpression on EGF-induced migration and on expression of putative target IEGs.
Fig. S4. Regulation of EGR1 by ID-miRs.
Fig. S5. Putative functions of predicted mRNA targets of EGF- and serum-regulated microRNAs.
Fig. S6. Examples of network motifs, including EGF-regulated microRNAs and co-occurring transcription factors (TFs).
Table S1. MicroRNA abundance analysis in MCF10A and HeLa cells treated with EGF or serum for the indicated time intervals.
Table S2. Clinical characteristics of breast cancer patients whose tumors were used for the analysis of microRNA abundance in EGFR/HER2-amplified vs. non-amplified tumors.
Table S3. Clinical characteristics of breast cancer patients whose tumors were used for the analysis of microRNA abundance in tumor vs. peritumor samples.
Table S4. Analysis of predicted targets of individual microRNAs.
Table S5. mRNAs induced by Dicer knockdown in starved MCF10A cells.
Table S6. Analysis of correlation between abundance of ID-miRs and abundance of predicted target IEGs in breast cancer patients.
Table S7. Analysis of correlation between microRNA abundance and that of predicted target genes.
Table S8. Analysis of enrichment of microRNA-TF pairs.
Table S9. Primers used for cloning and real-time PCR.
References

REFERENCES AND NOTES

1. M. J. Lazzara, D. A. Lauffenburger, Quantitative modeling perspectives on the ErbB system of cell regulatory processes. *Exp. Cell Res.* **315**, 717–725 (2009).
2. I. Amit, A. Citri, T. Shay, Y. Lu, M. Katz, F. Zhang, G. Tarcic, D. Siwak, J. Lahad, J. Jacob-Hirsch, N. Amariglio, N. Vaisman, E. Segal, G. Rechavi, U. Alon, G. B. Mills, E. Domany, Y. Yarden, A module of negative feedback regulators defines growth factor signaling. *Nat. Genet.* **39**, 503–512 (2007).
3. S. D. Santos, P. J. Verveer, P. I. Bastiaens, Growth factor-induced MAPK network topology shapes Erk response determining PC-12 cell fate. *Nat. Cell Biol.* **9**, 324–330 (2007).
4. I. Dikic, S. Giordano, Negative receptor signalling. *Curr. Opin. Cell Biol.* **15**, 128–135 (2003).
5. T. A. Berset, E. F. Hoier, A. Hajnal, The *C. elegans* homolog of the mammalian tumor suppressor Dep-1/Scc1 inhibits EGFR signaling to regulate binary cell fate decisions. *Genes Dev.* **19**, 1328–1340 (2005).
6. Y. Zwang, Y. Yarden, Systems biology of growth factor-induced receptor endocytosis. *Traffic* **10**, 349–363 (2009).

7. K. I. Patterson, T. Brummer, P. M. O'Brien, R. J. Daly, Dual-specificity phosphatases: Critical regulators with diverse cellular targets. *Biochem. J.* **418**, 475–489 (2009).

8. Y. Nakabeppu, K. Ryder, D. Nathans, DNA binding activities of three murine Jun proteins: Stimulation by Fos. *Cell* **55**, 907–915 (1988).

9. V. Baron, E. D. Adamson, A. Calogero, G. Ragona, D. Mercola, The transcription factor Egr1 is a direct regulator of multiple tumor suppressors including TGFβ1, PTEN, p53, and fibronectin. *Cancer Gene Ther.* **13**, 115–124 (2006).

10. I. Amit, R. Wides, Y. Yarden, Evolvable signaling networks of receptor tyrosine kinases: Relevance of robustness to malignancy and to cancer therapy. *Mol. Syst. Biol.* **3**, 151 (2007).

11. D. P. Bartel, C. Z. Chen, Micromanagers of gene expression: The potentially widespread influence of metazoan microRNAs. *Nat. Rev. Genet.* **5**, 396–400 (2004).

12. B. P. Lewis, C. B. Burge, D. P. Bartel, Conserved seed pairing, often flanked by adenosines, indicates that thousands of human genes are microRNA targets. *Cell* **120**, 15–20 (2005).

13. G. A. Calin, C. M. Croce, MicroRNA signatures in human cancers. *Nat. Rev. Cancer* **6**, 857–866 (2006).

14. T. C. Chang, D. Yu, Y. S. Lee, E. A. Wentzel, D. E. Arking, K. M. West, C. V. Dang, A. Thomas-Tikhonenko, J. T. Mendell, Widespread microRNA repression by Myc contributes to tumorigenesis. *Nat. Genet.* **40**, 43–50 (2008).

15. H. Y. Irie, R. V. Pearline, D. Grueneberg, M. Hsia, P. Ravichandran, N. Kothari, S. Natesan, J. S. Brugge, Distinct roles of Akt1 and Akt2 in regulating cell migration and epithelial-mesenchymal transition. *J. Cell Biol.* **171**, 1023–1034 (2005).

16. Cancer Genome Atlas Research Network, Comprehensive genomic characterization defines human glioblastoma genes and core pathways. *Nature* **455**, 1061–1068 (2008).

17. A. Shkumatava, A. Stark, H. Sive, D. P. Bartel, Coherent but overlapping expression of microRNAs and their targets during vertebrate development. *Genes Dev.* **23**, 466–481 (2009).

18. M. Kertesz, N. Iovino, U. Unnerstall, U. Gaul, E. Segal, The role of site accessibility in microRNA target recognition. *Nat. Genet.* **39**, 1278–1284 (2007).

19. L. F. Lau, D. Nathans, Expression of a set of growth-related immediate early genes in BALB/c 3T3 cells: Coordinate regulation with c-*fos* or c-*myc*. *Proc. Natl. Acad. Sci. U.S.A.* **84**, 1182–1186 (1987).

20. E. Hornstein, N. Shomron, Canalization of development by microRNAs. *Nat. Genet.* **38**, S20–S24 (2006).

21. R. Zenz, E. F. Wagner, Jun signalling in the epidermis: From developmental defects to psoriasis and skin tumors. *Int. J. Biochem. Cell Biol.* **38**, 1043–1049 (2006).

22. V. N. Kim, MicroRNA biogenesis: Coordinated cropping and dicing. *Nat. Rev. Mol. Cell Biol.* **6**, 376–385 (2005).

23. D. C. Hargreaves, T. Horng, R. Medzhitov, Control of inducible gene expression by signal-dependent transcriptional elongation. *Cell* **138**, 129–145 (2009).

24. V. R. Ramirez-Carrozzi, D. Braas, D. M. Bhatt, C. S. Cheng, C. Hong, K. R. Doty, J. C. Black, A. Hoffmann, M. Carey, S. T. Smale, A unifying model for the selective regulation of inducible transcription by CpG islands and nucleosome remodeling. *Cell* **138**, 114–128 (2009).

25. R. Saba, C. D. Goodman, R. L. Huzarewich, C. Robertson, S. A. Booth, A miRNA signature of prion induced neurodegeneration. *PLoS One* **3**, e3652 (2008).

26. E. Gottwein, N. Mukherjee, C. Sachse, C. Frenzel, W. H. Majoros, J. T. Chi, R. Braich, M. Manoharan, J. Soutschek, U. Ohler, B. R. Cullen, A viral microRNA functions as an orthologue of cellular miR-155. *Nature* **450**, 1096–1099 (2007).

27. S. Li, H. Fu, Y. Wang, Y. Tie, R. Xing, J. Zhu, Z. Sun, L. Wei, X. Zheng, MicroRNA-101 regulates expression of the v-fos FBJ murine osteosarcoma viral oncogene homolog (FOS) oncogene in human hepatocellular carcinoma. *Hepatology* **49**, 1194–1202 (2009).

28. F. van Straaten, R. Muller, T. Curran, C. Van Beveren, I. M. Verma, Complete nucleotide sequence of a human c-*onc* gene: Deduced amino acid sequence of the human c-*fos* protein. *Proc. Natl. Acad. Sci. U.S.A.* **80**, 3183–3187 (1983).

29. T. Sørlie, C. M. Perou, R. Tibshirani, T. Aas, S. Geisler, H. Johnsen, T. Hastie, M. B. Eisen, M. van de Rijn, S. S. Jeffrey, T. Thorsen, H. Quist, J. C. Matese, P. O. Brown, D. Botstein, P. Eystein Lonning, A. L. Børresen-Dale, Gene expression patterns of breast carcinomas distinguish tumor subclasses with clinical implications. *Proc. Natl. Acad. Sci. U.S.A.* **98**, 10869–10874 (2001).

30. A. Subramanian, P. Tamayo, V. K. Mootha, S. Mukherjee, B. L. Ebert, M. A. Gillette, A. Paulovich, S. L. Pomeroy, T. R. Golub, E. S. Lander, J. P. Mesirov, Gene set enrichment analysis: A knowledge-based approach for interpreting genome-wide expression profiles. *Proc. Natl. Acad. Sci. U.S.A.* **102**, 15545–15550 (2005).

31. V. K. Mootha, J. Bunkenborg, J. V. Olsen, M. Hjerrild, J. R. Wisniewski, E. Stahl, M. S. Bolouri, H. N. Ray, S. Sihag, M. Kamal, N. Patterson, E. S. Lander, M. Mann, Integrated analysis of protein composition, tissue diversity, and gene regulation in mouse mitochondria. *Cell* **115**, 629–640 (2003).

32. O. Hobert, Gene regulation by transcription factors and microRNAs. *Science* **319**, 1785–1786 (2008).

33. R. Shalgi, D. Lieber, M. Oren, Y. Pilpel, Global and local architecture of the mammalian microRNA–transcription factor regulatory network. *PLoS Comput. Biol.* **3**, e131 (2007).

34. U. Alon, in *An Introduction to Systems Biology—Design Principles of Biological Circuits*, C. Hall, Ed. (Chapman and Hall/CRC, Boca Raton, FL, 2006).

35. A. C. Mallory, H. Vaucheret, MicroRNAs: Something important between the genes. *Curr. Opin. Plant Biol.* **7**, 120–125 (2004).

36. A. Stark, J. Brennecke, N. Bushati, R. B. Russell, S. M. Cohen, Animal MicroRNAs confer robustness to gene expression and have a significant impact on 3′UTR evolution. *Cell* **123**, 1133–1146 (2005).

37. X. Li, R. W. Carthew, A microRNA mediates EGF receptor signaling and promotes photoreceptor differentiation in the *Drosophila* eye. *Cell* **123**, 1267–1277 (2005).

38. O. Shalem, O. Dahan, M. Levo, M. R. Martinez, I. Furman, E. Segal, Y. Pilpel, Transient transcriptional responses to stress are generated by opposing effects of mRNA production and degradation. *Mol. Syst. Biol.* **4**, 223 (2008).

39. E. A. Miska, E. Alvarez-Saavedra, A. L. Abbott, N. C. Lau, A. B. Hellman, S. M. McGonagle, D. P. Bartel, V. R. Ambros, H. R. Horvitz, Most *Caenorhabditis elegans* microRNAs are individually not essential for development or viability. *PLoS Genet.* **3**, e215 (2007).

40. B. Wang, A. Yanez, C. D. Novina, MicroRNA-repressed mRNAs contain 40S but not 60S components. *Proc. Natl. Acad. Sci. U.S.A.* **105**, 5343–5348 (2008).

41. E. Segal, N. Friedman, D. Koller, A. Regev, A module map showing conditional activity of expression modules in cancer. *Nat. Genet.* **36**, 1090–1098 (2004).

42. V. R. Iyer, M. B. Eisen, D. T. Ross, G. Schuler, T. Moore, J. C. Lee, J. M. Trent, L. M. Staudt, J. Hudson Jr., M. S. Boguski, D. Lashkari, D. Shalon, D. Botstein, P. O. Brown, The transcriptional program in the response of human fibroblasts to serum. *Science* **283**, 83–87 (1999).

43. D. F. Marrone, M. J. Schaner, B. L. McNaughton, P. F. Worley, C. A. Barnes, Immediate-early gene expression at rest recapitulates recent experience. *J. Neurosci.* **28**, 1030–1033 (2008).

44. V. Ramachandran, X. Chen, Degradation of microRNAs by a family of exoribonucleases in *Arabidopsis*. *Science* **321**, 1490–1492 (2008).

45. F. Meng, H. Wehbe-Janek, R. Henson, H. Smith, T. Patel, Epigenetic regulation of microRNA-370 by interleukin-6 in malignant human cholangiocytes. *Oncogene* **27**, 378–386 (2008).

46. L. Zhang, J. Huang, N. Yang, J. Greshock, M. S. Megraw, A. Giannakakis, S. Liang, T. L. Naylor, A. Barchetti, M. R. Ward, G. Yao, A. Medina, A. O'Brien-Jenkins, D. Katsaros, A. Hatzigeorgiou, P. A. Gimotty, B. L. Weber, G. Coukos, microRNAs exhibit high frequency genomic alterations in human cancer. *Proc. Natl. Acad. Sci. U.S.A.* **103**, 9136–9141 (2006).

47. U. Lehmann, B. Hasemeier, M. Christgen, M. Muller, D. Romermann, F. Langer, H. Kreipe, Epigenetic inactivation of microRNA gene *hsa-mir-9-1* in human breast cancer. *J. Pathol.* **214**, 17–24 (2008).

48. B. N. Davis, A. C. Hilyard, G. Lagna, A. Hata, SMAD proteins control DROSHA-mediated microRNA maturation. *Nature* **454**, 56–61 (2008).

49. M. Kato, S. Putta, M. Wang, H. Yuan, L. Lanting, I. Nair, A. Gunn, Y. Nakagawa, H. Shimano, I. Todorov, J. J. Rossi, R. Natarajan, TGF-β activates Akt kinase through a microRNA-dependent amplifying circuit targeting PTEN. *Nat. Cell Biol.* **11**, 881–889 (2009).

50. P. Bhat-Nakshatri, G. Wang, N. R. Collins, M. J. Thomson, T. R. Geistlinger, J. S. Carroll, M. Brown, S. Hammond, E. F. Srour, Y. Liu, H. Nakshatri, Estradiol-regulated microRNAs control estradiol response in breast cancer cells. *Nucleic Acids Res.* **37**, 4850–4861 (2009).